A Unifying Framework for Estimating Generation Time in Age-Structured Populations: Implications for Phylogenetics and Conservation Biology

(article starts on next page)

A Unifying Framework for Estimating Generation Time in Age-Structured Populations: Implications for Phylogenetics and Conservation Biology

Johan Jonasson,[1] Tero Harkonen,[2] Lisa Sundqvist,[3] Scott V. Edwards,[4] and Karin C. Harding[5,*]

1. Department of Mathematical Sciences, Chalmers University of Technology and University of Gothenburg, Gothenburg, Sweden;
2. Maritimas AB, Höga 160, 442 73 Kärna, Sweden;   3. Swedish Meteorological and Hydrological Institute, Gothenburg, Sweden;
4. Department of Organismic and Evolutionary Biology, Museum of Comparative Zoology, Harvard University, Cambridge, Massachusetts 02138;   5. Department of Biological and Environmental Sciences, Gothenburg University, Gothenburg, Sweden

ABSTRACT: Generation time is a measure of the pace of life and is used to describe processes in population dynamics and evolution. We show that three commonly used mathematical definitions of generation time in age-structured populations can produce different estimates of up to several years for the same set of life history data. We present and prove a mathematical theorem that reveals a general order relation among the definitions. Furthermore, the exact population growth rate at the time of sampling influences estimates of generation time, which calls for attention. For phylogenetic estimates of divergence times between species, included demographic data should be collected when the population growth rate for each species is most common and typical. In conservation biology, demographic data should be collected during phases of population decline in declining species, contrary to common recommendations to use predisturbance data. The results can be used to improve the International Union for Conservation of Nature's recommendation in parameterizing models for evaluating threat categories of threatened species and to avoid underestimating extinction risk.

Keywords: population dynamics, conservation biology, phylogenetics, demography, population extinction risk, theoretical biology.

Introduction

Generation time is a pivotal parameter in estimating the extinction risks of vulnerable species, and it is widely used in phylogenetic analysis in estimating divergence times of species. Consequently, it is important to estimate genera-

tion time in a consistent and replicable manner in many applications in evolutionary and conservation biology (Bird et al. 2020). A precise measure of generation time in age-structured populations has to account for both the survival of mothers up to the age of each breeding event and the number of offspring produced at each age class over the entire female life span. Thus, we need to estimate generation time as an average from demographic rates in age-structured populations.

The International Union for Conservation of Nature (IUCN) provides an international standard for evaluation of the status of species and populations (IUCN 2006, 2012; Cooke et al. 2018). One important criterion for classifying the vulnerability of a population into threat categories is the rate of decline over a time span of three generations. Thus, the estimated length of a generation influences the time period of assessment and thereby threat category and conservation efforts. An estimate of generation time that is too short will underestimate the threat facing a declining species, whereas an estimate that is too long will exaggerate the risk for extinction (Staerk et al. 2019). The importance of choosing a relevant method in estimating generation time in conservation biology has, to our knowledge, not been systematically reviewed, and guidance would be valuable for which of the possible measures to apply in given situations and which demographic data collected during population decline or growth should be used in estimating population threat categories.

The effective population size (N_e) of a species is a fundamental parameter with relevance to conservation biology and molecular evolution. Estimates of effective population sizes (Nei 1987; Nei et al. 1975; Nei and Takahata 1993) depend critically on the generation time parameter and can

* Corresponding author; email: karin.harding@bioenv.gu.se.

   ORCIDs: Jonasson, https://orcid.org/0000-0002-6028-9390; Edwards, https://orcid.org/0000-0003-2535-6217; Harding, https://orcid.org/0000-0003-1527-0903.

therefore vary with the definition of generation time (Bakker et al. 2022). For example, in the black-footed albatross (*Diomeida nigripes*), three different estimates of generation time, ranging from 7 to 20 years have been reported from field studies, which generated estimates of N_e ranging from 5,340 to 15,286 individuals (Cousins and Cooper 2000; Niel and Lebreton 2005; Dierickx et al. 2015). Ohta and Kimura (1971) famously invoked an inverse relationship between N_e and generation time to explain the constancy of the evolutionary rate of proteins, where substitution rates of deleterious mutations are influenced by N_e. This inverse relationship has been corroborated empirically (Chao and Carr 1993) and reminds us how important generation time is to our parameterization of molecular evolutionary rates.

The effect of generation time on molecular evolutionary rates also makes it central to estimate divergence times on phylogenies (Easteal 1985; Martin and Palumbi 1993; Mooers and Harvey 1994; Li et al. 1996). Age at first breeding is often used as a proxy for estimates of generation time (Weir and Schluter 2008; Lehtonen and Lanfear 2014; Gao et al. 2016), which obviously will bias results, underestimate true generation time, and consequently underestimate time since common ancestry and extinction risk. To estimate divergence times, we need data on the degree of genetic divergence between species, the substitution rate, and an estimate of generation time typical for the species or clade. However, how estimates of generation time are calculated can have a significant impact on the resulting estimates of divergence time. For example, Scally and Durbin (2012) assumed a fixed generation time of 25 years for humans and elaborated different estimates of the mutation rate in human evolution (from about 10^{-9} bp^{-1} to 1; 38×10^{-8} bp^{-1} per generation) and then showed how the estimated time for the split of Neanderthals and modern humans changed from about 350,000 to 500,000 years (Scally and Durbin 2012). However, generation times of modern humans in hunter-gatherer societies vary by as much as 10 years (Fenner 2005), a level of variation that strongly influences the estimated divergence times. The measure of generation time itself will introduce an additional variation of about 50% in the estimated divergence time of Neanderthals and modern humans, since annual mutation rates will change from 0.4×10^{-9} to 0.6×10^{-9} per year given a generation time of 20 versus 30 years (Scally and Durbin 2012). Furthermore, the contribution to the human mutation rate from the maternal and paternal sides is significantly different, with up to three times more mutations per year from the paternal side, which calls for even more detailed calculations of the contribution of each sex to the functional generation time for phylogenetic inference (Kong et al. 2012; Besenbacher et al. 2019; Taylor et al. 2019).

One reason why accurate measures of generation time often have been overlooked might be the seemingly simple means of calculating them. However, estimates of generation time are evasive when it comes to parameterization and require some mathematical attention. Age-structured population growth is correctly described in continuous time by renewal processes, and individual-level demographic variation can be portrayed using branching process theory (Jagers 1975), which is not commonly used by biologists. An initial simplifying approach of the population dynamics of seasonally breeding organisms is therefore to represent the demography with discrete time projection models, such as the Leslie matrix model (Leslie 1966). Fortunately, the discretization of population dynamics has proved to be a very good approximation of continuous time models (Fujiwara and Diaz-Lopez 2017), and we will build on that tradition here.

Estimating generation time from discrete data can be complicated and carried out in several ways. One method is the individual-centered estimate of "the mean age at births for a female during her lifetime" (denoted μ below). Another mathematical method can be phrased as a population-centered estimate: "the average age of mothers for a given cohort of newborns" (denoted A below). Over the past several decades, many theoretical articles have elaborated equations to capture measures of generation time (Dublin and Lotka 1925; Laughlin 1965; Leslie 1966; Jagers 1975; Lande 1988; Caswell 2001; Haccou et al. 2005; Bienvenu and Legendre 2015). We review common methods used for estimating generation time and categorize them into three different measures on the basis of their mathematical properties. We then give a strict mathematical proof of the relation between them. We also illustrate the performance of the three measures of generation time using biologically founded functions of vital rates from a range of species with contrasting life histories (Fujiwara and Diaz-Lopez 2017). We find that the resulting measures of generation time depend not only on the mathematical method applied but also on when the life history data were collected, in particular, the exact population growth rate at the time of collection.

The analyses presented here focus on age-structured populations described by Leslie matrices and do not extend to stage-structured populations. However, our analyses have quite broad relevance and are germane, for example, to most mammal and bird species, which typically have age-structured life histories (Caswell 2001), in addition to many other organisms from different taxa with life histories where age is used to model the population growth, such as sharks, many amphibians, and fishes (IUCN 2012). Among such populations are many red-listed species, where the exact measure of generation time is important in defining their threat status, as we discuss. We also give recommendations on which measure of generation time to apply and which life history data to collect, depending on the research question.

Material and Methods

Establishing Age-Structured Dynamics

Life histories for a species consisting of individuals with a maximum life span of n years can be specified by the Leslie matrix $\mathbf{L} = [l_{ij}]_{i,j=1,...,n}$, where the first-row elements $l_{1j} = f_j$ are the age-specific fertilities, that is, the expected number of offspring at age j of a (surviving) individual of age $j - 1$. The subdiagonal of the matrix, $l_{j+1,j} = s_j$, is the probability that an individual of age $j - 1$ survives to the age of j, and $l_{ij} = 0$ for all other matrix elements (i, j):

$$\mathbf{L} = \begin{pmatrix} f_1 & f_2 & \cdots & f_n \\ s_1 & 0 & \cdots & 0 \\ \vdots & \vdots & \ddots & \vdots \\ 0 & \cdots & s_{n-1} & 0 \end{pmatrix}.$$

The age-specific fertility f_j can itself be written as $s_j b_j$, where b_j is the fecundity at age j; that is, b_j is the expected number of offspring of an individual at age j given that she is alive at age j (unlike f_j, which conditions only on the individual being alive 1 year earlier).

To project the population forward in time, the matrix is multiplied with a column vector with the starting configuration $\mathbf{x}_0 = (x_0(1), ..., x_0(n))'$, where $x_0(j)$ is the number of individuals of age $j - 1$ at year 0. Then for each $t = 1, 2, ...$, the expected population configuration at time t is given by

$$\mathbf{x}_t = L^t \mathbf{x}_0.$$

Let $S_j = \prod_{i=1}^{j} s_i$, $j = 0, ..., n - 1$, be the probability that an individual survives until the age of j years and write

$$p_j = S_{j-1} f_j, \quad j = 1, ..., n.$$

Then, p_j is the expected number of offspring a newborn individual will generate at the age of j (note the difference between p_j and f_j; f_j is the conditional expected number of offspring at time j given that the individual is still alive at time $j - 1$, whereas p_j, the so-called net age-specific fertility, also takes into account the probability of surviving up to each specific age class). This is analogous to how f_j can be written as $s_j b_j$, where b_j is the fecundity at age j, with the difference that f_j takes into account survival probability from age $j - 1$ to j, whereas p_j takes into account survival the whole way from being a newborn to age j.

Let λ be the largest real eigenvalue of $\mathbf{L}$. The population size will roughly grow with a factor λ per year.

Strict and Self-Looped Leslie Matrices

For the sake of convenience, it is common to decrease the size of the Leslie matrix in analyzing the dynamics of long-lived species by treating all adults as one single class and apply a so-called extended or self-looped Leslie matrix. To represent that, an element $s_n > 0$ is added to produce a self-loop (n, n) on the original Leslie matrix, with the consequence that an individual, after reaching age n, has probability s_n of surviving and breeding again. The classical generation time measures discussed here can not be calculated from life history data presented in the self-looped Leslie matrix format; however, it is straightforward to first transfer any looped Leslie matrix to a strict Leslie matrix and then apply the estimates and reasoning presented here.

We recommend that, in calculating generation time, extended Leslie matrices shall first be rewritten in the format of the strict Leslie matrix by expanding the matrix dimension to let one row and column represent each age class—for example, set n to be the maximum longevity of the species. With modern software, computation times involving matrices of the size that we are dealing with here are virtually instantaneous.

Common Estimators of Generation Time

We performed a literature survey and compiled functions from seven well-cited articles on estimating generation time by different methods in age-structured populations, and notations were rewritten to enable comparisons among the different measures (Dublin and Lotka 1925; Laughlin 1965; Leslie 1966; Coale 1972; Charlesworth 1994; Lebreton 1996; Caswell 2001). It turned out that many of the equations were the same and had been invented repeatedly. We find three main methods to estimate generation time; the first is here denoted by T (Dublin and Lotka 1925; Laughlin 1965; Leslie 1966; Coale 1972; Charlesworth 1994), the second by μ (Leslie 1966; Coale 1972; Charlesworth 1994; Lebreton 1996; Caswell 2001), and the third by A (Leslie 1966; Coale 1972; Charlesworth 1994; Caswell 2001). These three most common measures of generation time are defined as follows.

The first measure is the time T taken for the population to grow (or decline) by a factor that equals the expected total number of offspring per female, $R_0 = \sum_{j=1}^{n} p_j$, at the current population growth rate (λ); that is,

$$T = \frac{\log R_0}{\log \lambda}.$$

This is equivalent to dividing a number by a rate and thus obtaining the time.

The second measure is the mean age at reproduction, μ, of an average mother over her lifetime (i.e., the mean age difference between an average individual and her daughters):

$$\mu = \frac{\sum_{j=1}^{n} j p_j}{\sum_{j=1}^{n} p_j}.$$

The third measure is the mean age A of the mothers of the offspring that are born a given year. Here, the contribution from reproduction at a given age is scaled by the relative abundance of each age class in the population through multiplication with λ^{-j}. This is a population-centred generation time (further simplified below):

$$A = \frac{\sum_{j=1}^{n} j\lambda^{-j} p_j}{\sum_{j=1}^{n} \lambda^{-j} p_j}.$$

According to general linear algebra, an eigenvalue of $\mathbf{L}$ is a number θ that satisfies the characteristic equation $\det(\theta\mathbf{I} - \mathbf{L}) = 0$, which in this case turns out to be

$$\theta^n - \sum_{j=1}^{n} \theta^{n-j} p_j = 0. \tag{1}$$

This equation is equivalent to the standard Euler-Lotka form

$$\sum_{j=1}^{n} \theta^{-j} p_j = 1.$$

Hence, λ is the largest real solution to this equation. Moreover, the left-hand side of the Euler-Lotka equation is decreasing for $\theta \geq 0$, so λ is the unique nonnegative real solution and $\sum_{j=1}^{n} \theta^{-j} p_j \geq 1$ implies $\theta \leq \lambda$ and vice versa.

The definition of A now simplifies to

$$A = \sum_{j=1}^{n} j p_j \lambda^{-j}.$$

It is obvious that $\lambda = 1$ if and only if $R_0 = \sum_{j=1}^{n} p_j = 1$. Note that T is not defined when $\lambda = 1$. We suggest that it would be natural to define T for $\lambda = 1$ by taking a limit as $p' = (p'_0, \dots, p'_{n-1})$ converges to $p = (p_0, \dots, p_{n-1})$ in such a way that $R_0(p') \neq 1$. However, it has not been clear that the limit exists or is well defined. One consequence of theorem 1 below is that the limit indeed exists and is independent of the precise form of p'.

Results

Mathematical Result

The mathematical relationship between the three different methods for estimating generation time is analyzed. The resulting mathematical proof makes repeated use of Jensen's inequality (Jensen 1906), which is related to the definition of a convex function; the proof of theorem 1 is presented in the appendix. The proof generates a theorem that holds for all Leslie matrix parameterizations of the three generation time definitions, A, μ, and T. The theorem shows that the magnitudes of the estimates of the three generation time measures follow a strict pattern that is given by the population growth rate (λ).

THEOREM 1. If $\lambda > 1$, then

$$A \leq T \leq \mu,$$

and if $\lambda < 1$, then

$$A \geq T \geq \mu.$$

If $\lambda = 1$, then T can be well defined as a limit as $\lambda \to 1$, and when doing so

$$A = T = \mu.$$

In plain words, in a growing population, method A produces the lowest estimate of generation time, followed by T and μ. In a declining population, A gives the highest estimate of generation time, and T and μ produce gradually lower estimates. When the population is stable, all three methods produce identical measures of generation time. The relation $A \leq \mu$ if and only if $\lambda > 1$ is intuitive, since estimate A takes the population age distribution into account (by scaling with population growth rate, λ^{-j}) and in a growing population the proportion of young individuals will be relatively larger than the proportion of older individuals, producing a lower generation time. By contrast, the mother-centered method μ does not compensate for the distribution of age classes in the population because it focuses solely on the average age of mothers at birth over their lifetime.

Fecundity and Survival Functions

To illustrate these mathematical results and their potential biological importance, we collected some simplified and some biologically motivated classic survival and fecundity functions (Bielby et al. 2007; Fujiwara and Diaz-Lopez 2017) and parametrized the Leslie matrix with them. We elaborated four different shapes of the fecundity functions $f(t)$, $t \geq 0$ (fig. 1), here described in continuous time because it is natural to define fecundity and survival functions for all times and not only integer-valued time points. One is age independent, and thus fecundity is constant: $b(t) = \gamma$. The second function represents a case with delayed maturity, that is, no offspring during the first years until a given age of maturity and thereafter constant fecundity (an abrupt fecundity function). We also apply one exponentially decreasing and one gradually increasing fecundity function:

$$b(t) = \gamma e^{-\kappa t} \tag{2}$$

and

$$b(t) = \gamma(1 - e^{-\kappa t})^3. \tag{3}$$

Function (3) starts at zero at age $t = 0$ and then gradually increases with rate κ (the rate of increase toward full maturity) to very close to γ ($b_{\text{adult}} = \gamma$, the steady-state fecundity
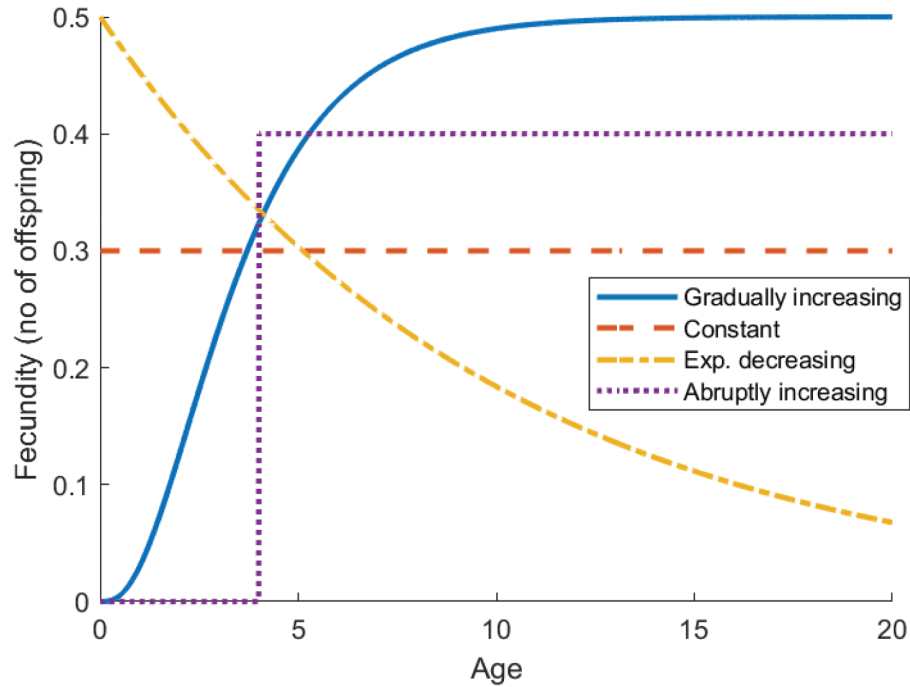
Figure 1: The different fecundity functions used to illustrate variation in estimates of generation time in figures 3–7.

of an adult). By manipulation of the exact values of κ and γ, these functions can represent a multitude of life histories. For example, by function (3) we obtain a *K*-strategist, pinniped-style fecundity function with $\gamma = \kappa = 0.5$, as illustrated in figure 1.

Three examples of survival functions $S(t)$ were also implemented. But first let us consider common terms that are inconsistently defined across authors and disciplines: hazard rate, mortality rate, and survival rate. The survival rate at age j, where $j \geq 0$ is an integer, is taken to be the probability that an individual of age $j - 1$ survives to the age of j (i.e., the survival rate at time j is simply the element s_j of the Leslie matrix). The mortality rate is then 1 minus the survival rate, $1 - s_j$. These interpretations are the most common in applied biology, whereas in mathematics the term "rate" would typically not be used for a quantity that is discrete in nature. The term "hazard rate" will in the following be taken to mean the mortality in continuous time. Writing $h(t)$ for the hazard rate at time t, this becomes

$$h(t) = -\frac{S'(t)}{S(t)}.$$

Conversely, this means for survival rate s_j that

$$s_j = \frac{S(j)}{S(j-1)} = e^{-\int_{j-1}^{j} h(t)\, dt}.$$

If the hazard rate is small, then

$$1 - s_j \approx h(j),$$

(i.e., the hazard rate and the mortality rate are close to equal).

The first two examples of survival functions are

$$S(t) = e^{-\alpha(e^{\beta t} - 1)} \tag{4}$$

and

$$S(t) = e^{-\alpha t}. \tag{5}$$

These correspond to an exponentially increasing hazard rate, $h(t) = \alpha \beta e^{\beta t}$, and a constant hazard rate over age, $h(t) = \alpha$, respectively. Hence, the first of these survival functions corresponds to senescence (i.e., increased mortality risk with age). For a population with constant hazard rate α, the yearly survival probability is $s = e^{-\alpha}$ or, equivalently, $\alpha = -\log(s)$.

The third survival function investigated is

$$S(t) = e^{-\alpha t} e^{-\beta(1 - e^{-\rho t})}, \tag{6}$$

which corresponds to high mortality in juvenile age classes, after which the hazard rate gradually decreases and converges to a constant value at high age. This type of pattern is seen in many *K*-strategists, such as marine mammals, humans, and long-lived plants. The corresponding hazard

rate is $\alpha + \beta\rho e^{-\rho t}$. The hazard rates associated with these survival functions are illustrated in figure 2.

In the following, we elaborate different combinations and parameter values of these functions to illustrate how much the corresponding estimates of generation time can vary (figs. 3–7).

Estimating Generation Time for Major Life History Types

Here, we calculate the generation time with the three methods A, μ, and T for different combinations of survival and fecundity, and for each combination the resulting population growth rate λ is noted. We first give a case where survival does not vary over age but is kept at 0.8 throughout life, and only the age-independent fecundity is increased stepwise, from 0.1 to 0.5, to obtain a range of matrices with different population growth rates (fig. 3a, x-axis). Here, the estimate of generation time μ remains constant at 4.77 across all parameterizations (fig. 3a); this illustrates that the mother-centered estimate μ does not respond to the increasing population growth rate, as long as the survival rate is constant across age classes and fecundity is evenly distributed over life, because average age at birth from the mothers perspective remains the same. On the other hand, the population-level generation time A declines with increasing population growth rate, since A depends on the population growth rate (i.e., at higher population growth rates we have more young

mothers in the population, which leads to a lower population-level generation time; fig. 3a). The estimate T is always intermediate.

However, if instead fecundity is kept constant, $b_j = \gamma = 0.5$, across age classes and only survival is adjusted to produce different growth rates, the mother-centred generation time estimate μ increases (since now a mother lives longer and gives birth to more offspring at later age). Instead, the population-based estimate A is constant at 2.96 years across all population growth rates (fig. 3b). This result follows because the increasing average age of mothers at birth is counteracted at the population level by the steeper age structure in the growing population in estimate A; in this special case, the two forces exactly counterbalance each other. The general pattern is that generation time A is always smaller than μ at positive population growth rates and typically declining with population growth rate for biologically realistic life histories (figs. 3–7). Figure 3a and figure 3b provide a baseline in the following discussion and show how different the mother-based generation time and the population-level generation time respond to the change in population age structure that comes with increasing growth rates. In the following, we study how a range of different interesting age dependencies in the demographic rates influences generation time.

Next, the age-dependent, gradually increasing fecundity function (eq. [3]) is explored, and the survival rate is kept constant (fig. 4a, 4b). The shape of the age-dependent
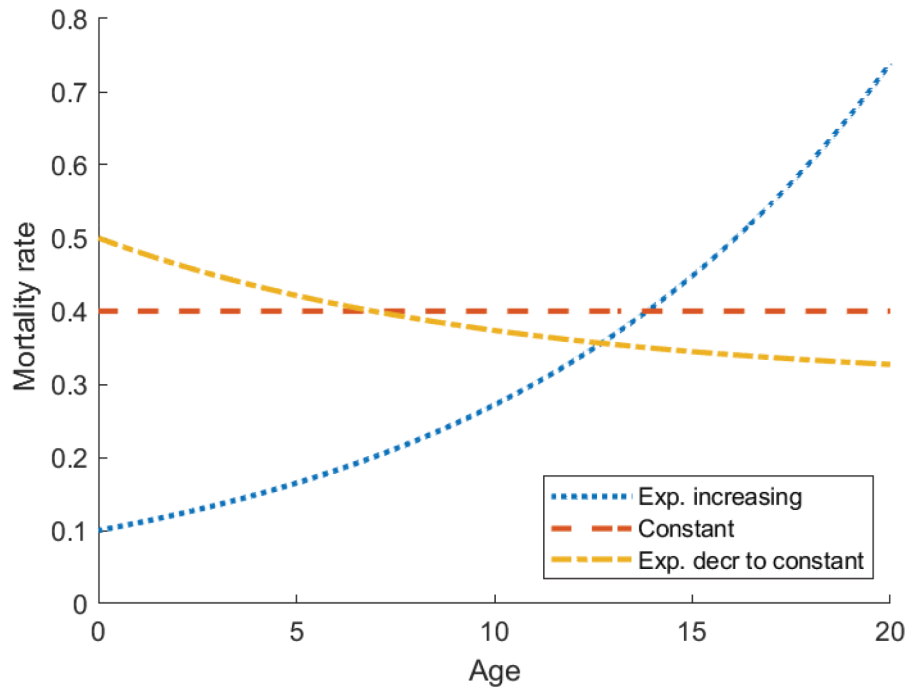

Figure 2: Hazard rates used to illustrate variation in estimates of generation time in figures 3–7.
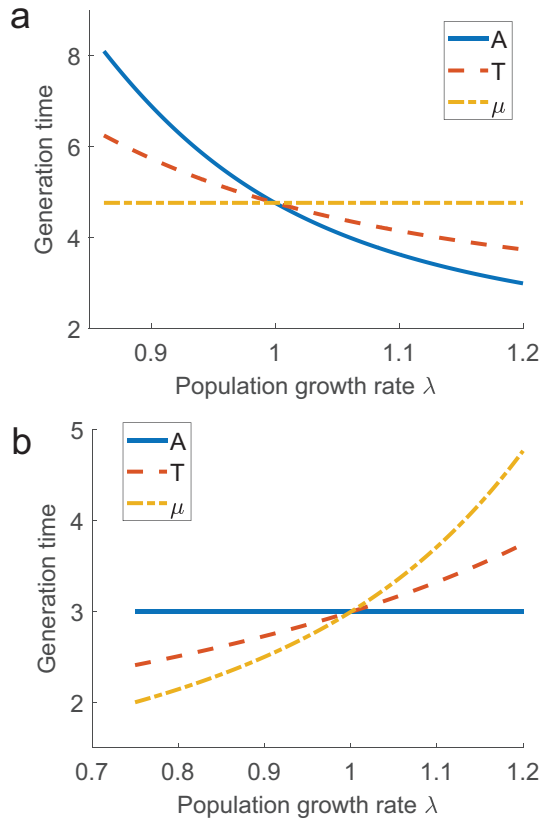
a

b

Figure 3: Estimates of generation time for life histories with constant survival and constant fecundity across age classes. For each combination of survival and fecundity values, the generation time (*y*-axis) is calculated with the three different methods (*A*, μ, and *T*), and the resulting population growth rate is given on the *x*-axis. The life histories plotted in *a* all have a survival rate of 0.8 while the average age-independent fecundity is gradually increased from 0.1 to 0.5, thereby giving rise to a range of growth rates for these hypothetical life histories. In *b*, fecundity is kept constant at 0.5 for all life histories plotted while the survival rate is gradually increased from 0.5 to 0.8 to obtain the range of growth rates.

fecundity function was varied in two different ways, first by manipulation of the adult fecundity γ (eq. [3]; fig. 4*a*) and second by changing the age at sexual maturation κ (eq. [3]; fig. 4*b*). The resulting pattern of generation time estimates in the first case resembles figure 3*a* and is explained in the same way: the mother-based average generation time μ is not influenced by population growth rate when the fecundity function over age maintains its shape. However, when age at sexual maturation κ is decreased to generate the higher population growth rates, all measures of generation time decline rapidly (fig. 4*b*).

In figure 5*a*, the age-dependent fecundity function (eq. [3]) is maintained the same in all calculations, and only the pattern of survival is changed. By increasing survival symmetrically for all age classes (fig. 5*a*) we get an almost identical

pattern in generation time estimates as in figure 3*b* (again, the mother-based estimate μ produces a greater generation time when survival increases, but this is counterbalanced by the younger age structure reflected in the population-based generation time estimate *A*). Next, we tweaked the fecundity function to illustrate a large difference among generation time estimates for a theoretical life history with reproduction only very early and very late in life (fig. 5*b*). When reproduction is distributed in this skewed way over a lifetime, the estimates of generation time produce results differing widely, by up to 10 years for the same data (i.e., for the same population growth rate in the graphs). Again, μ does not respond to increasing growth rates, since the distribution of birth over life is kept constant, whereas the population-based generation time *A* declines sharply, reflecting the younger age structure in a growing population (fig. 5*b*).
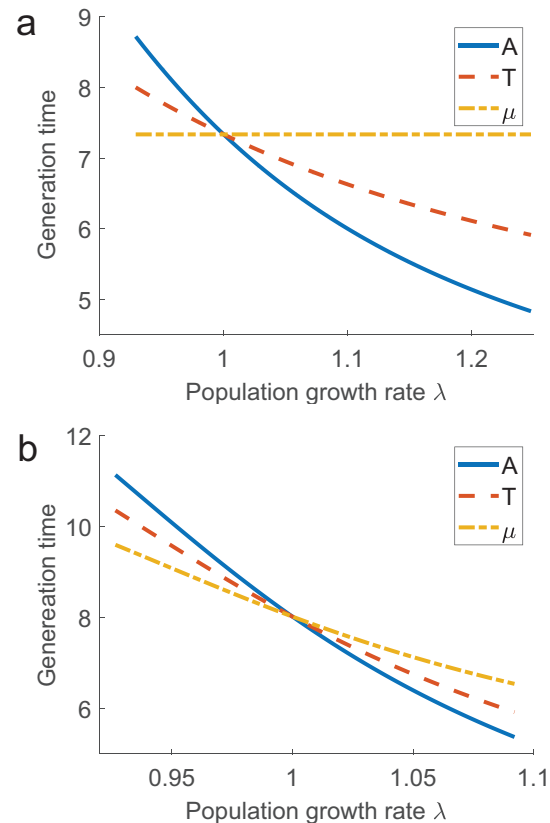
a

b

Figure 4: Measures of generation time for life histories with age-dependent, gradually increasing fecundity (fecundity function given by (3), illustrated in fig. 1). The survival rate is kept age independent, that is, constant at $\alpha = 0.8$ in both graphs. In *a*, fecundity values are derived with a fixed value on the rate of maturation $\kappa = 0.4$, and the adult fecundity γ is varied between 0.3 and 2.0 in order to obtain the different growth rates λ. In *b*, we have instead a fixed $\gamma = 0.7$, and κ is varied between 0.15 and 0.6.
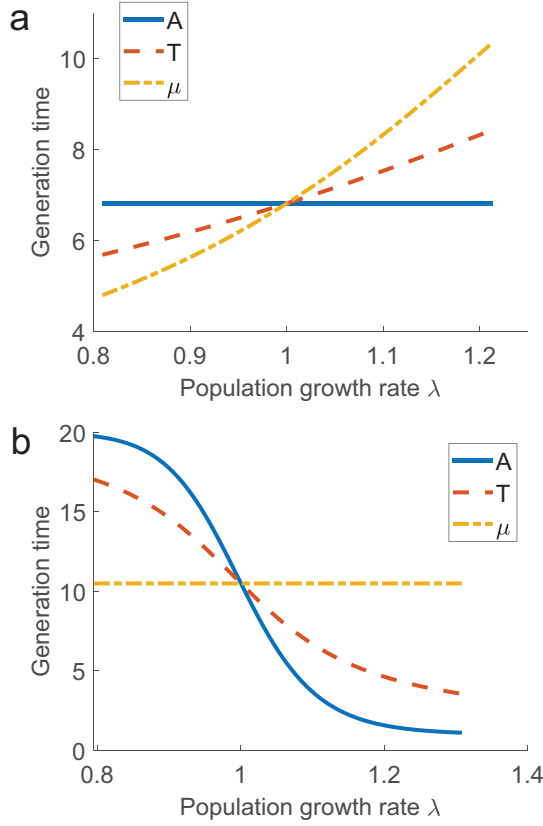
Figure 5: In *a* we again use the age-dependent fecundity function (3) with parameters kept fixed at $\gamma = 1.2$ and $\kappa = 0.3$. Instead, population growth rate varies as the age-independent survival rate α varies between 0.6 and 0.9. In *b*, a theoretical life history with extreme difference between the measures of generation time is shown. (Constant survival rate at 1, reproduction only at the ages of 1 and 20 years and $f_1 = f_{20} = \beta$, and λ varies as β ranges from 0.01 to 1.3.)

When instead survival rates are made age dependent, we have senescence. If that type of survival function is kept constant across runs and only fecundity is varied, generation time measures are not affected much and figure 6*a* is similar to figure 3*a*. When instead the degree of senescence itself is manipulated, we can obtain a pattern where the population-based generation time also increases with the population growth rate (fig. 6*b*). This pattern arises because, as the degree of senescence declines (going from left to right in the graph), the proportion of older individuals in the population also increases, causing all measures of generation time to increase (fig. 6*b*, right-hand side).

Figures 4–6 focus on various cases of life histories with early maturation, different reproductive outputs, and different survival rates, whereas figure 7 illustrates life histories with delayed maturation. All functions in figures 1 and 2 were investigated, although results are not illustrated be-cause the main patterns described above were also repeated when a more abrupt function for maturation was applied. We note that in some cases the three measures of generation time differ very little, whereas in other cases the differences are quite large. The general patterns depend on how the population age structure changes with growth rate to influence A.

We used $n = 20$ as the number of age classes in figures 3–6, which is sufficient to theoretically illustrate the phenomena that can occur, but this needs to be adjusted to the maximum life span of every study species. In figure 7, $n = 40$ is the number of age classes, which is the longevity of a ringed seal.
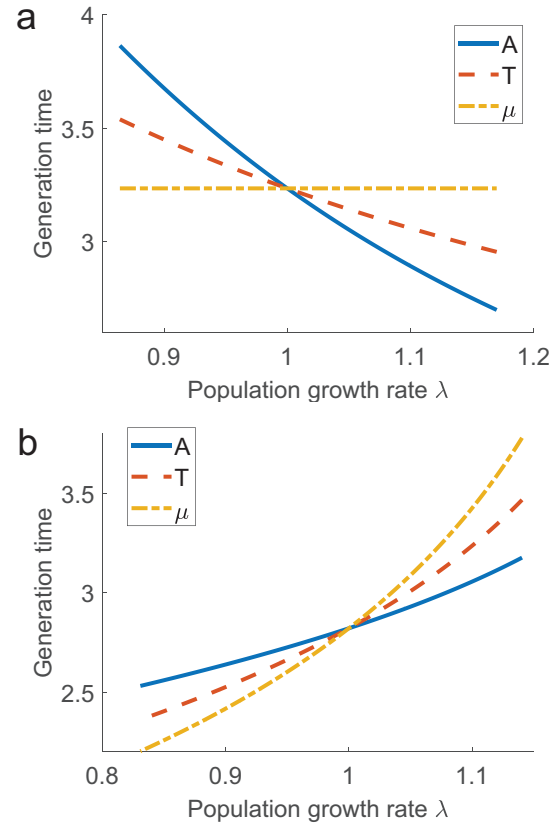

Figure 6: Here, the fecundity γ is constant over time in both plots, and survival rates are age dependent and declining with age, as given by $S_j = e^{-\alpha(e^{\beta j}-1)}$, corresponding to senescence (yellow curve in fig. 2, "exponentially decreasing to constant"). In *a*, this survival function is kept fixed with $\alpha = 0.25$ and $\beta = 0.3$. The population growth rate λ is varied by having offspring numbers γ across hypothetical populations between 0.15 and 0.4. In *b*, we instead keep the fecundity γ fixed at 0.3, while the shape of the survival function is varied as α varies between 0.1 and 0.5 and β is fixed at 0.35. Thus, the degree of senescence declines going from left to right in the graph, producing a gradually older age distribution in the populations and thus also a higher generation time for the population-based estimate A.
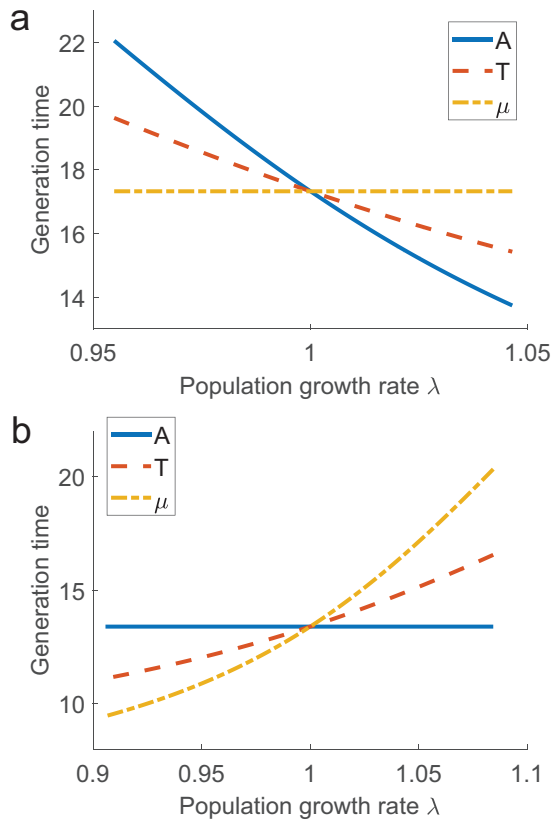
a

b

Figure 7: Measures of generation time of a pinniped-type life history, with delayed maturation; the fecundity is zero until the age of reproduction, where it increases to the constant γ (fig. 1, "abruptly increasing"). The survival probabilities reflect higher mortality at young ages, which then decreases to a small constant α (for the corresponding hazard rate, see fig. 2, "exp. decr to constant"). This choice of fecundity and survival functions reflects the life history of a pinniped and is here parameterized for the ringed seal (*Phoca hispida*). In a, $\alpha = 0.05$, $\beta = 1.2$, and $\rho = 0.7$, and λ varies as a function of γ, ranging from 0.1 to 0.5. In b, instead $\beta = 0.9$, $\rho = 0.7$, and $\gamma = 0.4$, and α ranging from 0.2 to 0.02. The life histories in this figure span 40 years, which is the maximum life span of ringed seals.

The Ringed Seal: A Case Study

Consider the ringed seal (*Phoca hispida*), which is found throughout the polar Arctic, as a concrete example of the consequences of applying different estimates of generation time. The ringed seal is an extreme *K*-strategist with low reproduction rate and high survival. Female ringed seals give birth to, at most, one pup annually, and age at first parturition is about 5 years (McLaren 1958; Smith 1973; Fedoseev 1975; Smith and Hammill 1981; Holst and Stirling 2002). First-year survival (s_1) is often about 0.5, annual subadult survival (s_2, s_3, s_4) is about 0.9, and annual adult survival ($s_5, \ldots, s_n$) is often estimated to about 0.95. These values result in an exponential rate of population growth (λ) at 1.1, a growth rate close to the maximum growth rate observed

for this and similar pinnipeds under favorable conditions (Harkonen et al. 2002; Harding et al. 2007). Lower values of population growth rates are common and often caused by food limitation, infectious diseases, and other disturbances (Harding et al. 2002, 2007; Silva et al. 2021). Poor nutritive condition influences a suite of changes in life history traits, following a typical sequence where pup survival is lowered first, followed by increased age at first reproduction of females, increased subadult mortality, and declining adult fertility; adult mortality is often the last parameter to be affected (Kjellqvist et al. 1995). Figure 7 illustrates how the three measures of generation time are affected by changes in these life history parameters. Here, survival probabilities are modeled by one of the standard functions given by Fujiwara and Diaz-Lopez (2017) closely resembling the survival functions for the ringed seal. Thus, the generation time varies from 14 to 22 years according to measure A depending on whether life history values are sampled under exponential growth or decline. The estimated generation time depends on whether the life history responds to better conditions with improved reproduction (fig. 7*a*) or increased survival rate (fig. 7*b*). The mother-based estimator μ does not change at all when reproduction is increased over all age classes (fig. 7*a*), whereas it increases as female survival is improved (fig. 7*b*).

Discussion

We focused on three commonly used approaches for estimating generation time represented by the definitions of T, μ, and A. We found that the choice of method has significant consequences for the resulting estimate (of up to several years) and that estimates also depend on the species' life history type. Furthermore, our results call for attention in the selection of demographic data from a given population, since generation time estimates depend on the population growth rate at the time of collection.

The general connection between generation time and population growth may not be immediately intuitive, but it is central to the dynamics displayed by the three measures of generation time we have considered here. As our analyses show, population growth can cause estimates of generation time to increase or decrease, depending on the pattern of age-specific fecundity and mortality rates giving rise to population growth. At the most general level, changes in population growth influence generation time because they change the age distribution of mothers, as is reflected in measures A and T, or the distribution of differences in age between mothers and daughters, as in estimate μ. But population growth and generation time do not display a simple correlation in terms of their effect on generation time. For example, when population growth rate is increased by increasing the fecundity alone but symmetrically over all age classes, the mother-based estimate μ is unaffected, since the average

age at birth for an individual mother remains the same. By contrast, if growth is increased by changing survival rate alone, then in fact μ may increase (each female becomes older and also has a chance to breed at later age classes), while A may decrease, since the population-based estimate A also captures the younger age structure in a rapidly increasing population. Thus, the varied influences from life history arise because of the influence (A and T) or lack of influence (μ) of population growth on the age distribution used by each estimator. In general, the effects of population growth on generation time are very dependent on the form of the survival and fecundity functions and their parameters (figs. 1, 2), and these will influence the dependence of generation time on population growth rate as well as the behavior of the different estimators of generation time.

The generation time estimate A describes the situation at the population level, taking the current population age structure into account, and is most accurate to use in applications of conservation biology and evolution. However, one can ask whether there are situations where μ is preferred over A. One case could be when studying individual reproductive schedules and how they change over time. For example, in pinnipeds, years with low food availability also cause delayed age at sexual maturity and year skipping in adult females; this will influence the mother-based generation time. A general point is perhaps that the mother-based definition μ is the easiest to understand intuitively and also to calculate, whereas A and T both require some more reflection and matrix manipulations. Also, in practice the coefficients of the Leslie matrix have to be estimated, for example, by following a sufficiently large number of females through their life span. These estimates then of course come with a variance, which causes variance in the estimates of μ, A, and T. It could be that the variance of A is typically higher than the variance of μ, as there is one more estimated parameter (namely, λ) in the formula for A than in the formula for μ. It would be interesting to see whether this is actually true for a reasonable model for the probability distribution of the observed data.

We suggest that method A should be the measure of choice for general use, since this estimate is based on the age difference between an average individual and her mother, which is the mean time between genetic recombination events and is hence the most relevant measure from a phylogenetic standpoint when considering the divergence time among species. For example, consider a population where all individuals survive until the age of 3 and then die and where the fecundity is 1 for 1- and 3-year-olds and 0 for individuals of age 2. Such a population will be exponentially increasing with a stationary age structure, for which there are more than twice as many 1-year-olds as 3-year-olds. Hence, the mean of age of an individual's mother will be less than 5/3, which is reflected by A, whereas for the estimator μ it equals 2. For species that are K-strategists, such as whales or seals, it might be the case that the population growth rate is typically close to 1 over evolutionary timescales. However, for a species where population growth is typically high during times between collapses (r-strategists such as rodents), the difference might be large, and it is important to use the most relevant method.

Implications for Phylogenetics

In recent years, there has been increased appreciation of the linkages between life history traits, generation time, and genome evolution. The generation time hypothesis, which states that variation in rates of molecular evolution over time and across lineages can be expected as generation time varies, has been a staple of molecular evolution for decades (Sarich and Wilson 1973; Easteal 1985; Wu and Li 1985). More recently, increased genome data have revealed dramatic signatures of generation time, effective population size, and life history traits on genomic traits, such as genome size, GC content, and rates of evolution (Romiguier et al. 2010; Figuet et al. 2016). The results presented here suggest that increased attention to variables influencing generation time is warranted, particularly given the increased detail with which we can now estimate changes in population size and growth through time (Li and Durbin 2011; Bakker et al. 2022) as well as sex differences in germline mutation rates per generation (Kong et al. 2012; Gao et al. 2016). Estimating divergence times, effective population sizes, and population dynamics between species is critically dependent on accurate estimates of generation time (Stoffel et al. 2018; Bakker et al. 2022), yet the connections between population dynamics and generation time have been little explored in the context of molecular dating. For example, more work is needed to explore the effective generation time of a phylogenetic lineage whose population growth varies over time. More detailed models of generation time will better serve the flood of genome data that allows increasingly precise connections between molecular rates, genome characteristics, and population and life history dynamics (Nadachowska-Brzyska et al. 2015; Wu et al. 2021).

Estimates of divergence times of species are ultimately based on estimates of generation times and effective population sizes. However, such estimates are often based on life history data from contemporary populations, which can be under transient phases of growth. For example, estimated generation times for minke whales (*Balaenoptera acutorostrata*) range between 7 years (Skaug 2001) and 17 years (Kishino et al. 1991), and these measures have been arbitrarily used in estimates of divergence times of species (e.g., Pastene et al. 2007). Similarly, life history data from populations of humpback whales (*Megaptera novaeangliae*), where estimates of generation time estimates range between 12 years (Chittleborough 1965) and 24 years (Pastene et al. 2007) among populations, have been used for analyses of historical events

(Roman and Palumbi 2003; Jackson et al. 2009). Data from current populations are commonly used in evolutionary genetic analyses in most other species, including birds (Sæther et al. 2005) and seals (Palo et al. 2003; Harkonen et al. 2005).

Implications for Conservation Biology

The conservation status of a species or population can be evaluated according to an IUCN criterion for the magnitude of population decline measured over (the longer of) 10 years or three generations. Threat categories are critically endangered (CR) for more than 90% decline in the given time period, endangered (E) for more than 70% decline, and vulnerable (V) for more than 50% decline in three generations. The IUCN also proposes the following stricter definition and recommendation: "Generation length is the average age of parents of the current cohort (i.e., newborn individuals in the population). Generation length therefore reflects the turnover rate of breeding individuals in a population. Generation length is greater than the age at first breeding and less than the age of the oldest breeding individual, except in taxa that breed only once. Where generation length varies under threat, the more natural, i.e. pre-disturbance, generation length should be used" (see https://www.iucnredlist .org/resources/categories-and-criteria, ver. 3.1). This definition is exactly the definition of A in the current study, and thus our analysis support the IUCN's recommendation in the choice of method. However, our conclusion from the analysis is the opposite when it comes to the parametrization with demographic data. Declining populations often show longer generation times, as we have illustrated for measure A in theorem 1 and the figures (e.g., see the ringed seal example in fig. 7*a*). Longer generation times lead to larger recorded declines in population size over time and thus give a more accurate estimate of the threat to a vulnerable species compared with "predisturbance" demography (which is often characterized by higher reproductive rates and shorter generation time). Thus, the precautionary principle (Kriebel et al. 1981) would suggest the use of generation time measure A parametrized with demographic data from the contemporary declining population.

Conclusion

Three classical main approaches for estimating generation time produce different estimates for the same life history data. We provide a mathematical theorem showing the relative order of magnitude of the estimates, and we illustrate the problem for many biologically realistic situations. It is important to carefully select both method and the empirical life history data for parametrization, since estimates of generation time can be biased by up to several years. Such errors magnify if used in phylogenetic studies of time since common

ancestry and can also bias estimates of the population extinction risk of red-listed species. We propose one method over the other two, which is population based and equivalent to the average age of breeding females a given year, and discuss how it shall be parameterized with demographic data depending on research question.

Statement of Authorship

T.H. identified the original research question. J.J. and K.C.H. conceptualized the project idea and developed the mathematical analysis. J.J., T.H., L.S., K.C.H., and S.V.E. wrote the final version.

Data and Code Availability

All code to re-create the results and figures can be found in Zenodo (https://doi.org/10.5281/zenodo.6600015; Jonasson 2022) and in GitHub (https://github.com/jonasson66 /Generation-times).

APPENDIX

Proof of Theorem 1 and Remarks

Recall the definitions of the three common methods for estimating generation time, μ, A, and T:

$$T = \frac{\log R_0}{\log \lambda},$$

$$\mu = \frac{\sum_{j=1}^{n} j p_j}{\sum_{j=1}^{n} p_j},$$

$$A = \frac{\sum_{j=1}^{n} j \lambda^{-j} p_j}{\sum_{j=1}^{n} \lambda^{-j} p_j},$$

where p_j is the expected number of offspring a newborn individual will have at age j, R_j is the expected total number of offspring an individual will have during her lifetime, and λ is the unique real eigenvalue of the Leslie matrix.

Since A differs from μ by the weight λ^{-j} to term j, it is obvious that $A \leq \mu$ for $\lambda > 1$ and the reverse when $\lambda < 1$ is also obvious. However, that T is sandwiched between them is not at all obvious and has to the best of our knowledge not been strictly proven before. To prove it, we will make repeated use of Jensen's inequality, which is a standard

result of probability theory, stating that for any convex function g and any random variable such that $\mathbb{E}[X]$ and $\mathbb{E}[g(X)]$ both exist,

$$\mathbb{E}[g(X)] \geq g(\mathbb{E}[X]).$$

Recall also that a function g is said to be convex if for any x_1, x_2 and any $a \in [0, 1]$, $g(ax_1 + (1 - a)x_2) \leq ag(x_1) + (1 - a)g(x_2)$. In particular, if g is twice differentiable, then g is convex if and only if $g''(x) \geq 0$ for all x.

Let us first prove the relation between T and μ. We will use that $\log R_0 / \log R_0^{1/\mu} = \mu$ so that since $T = \log R_0 / \log \lambda$, it suffices to show that $\lambda \geq R_0^{1/\mu}$. For that, we use Jensen's inequality. Observe that for any number $a > 0$, the function $x \rightarrow a^x$ is convex, so for any random variable X, Jensen's inequality tells us that $\mathbb{E}[a^X] \geq a^{\mathbb{E}[X]}$. Use this with X being the random variable for which $\mathbb{P}(X = n - j) = q_j$, where $q_j = p_j/R_0$, $j = 1, \dots, n$, and $a = R_0^{1/\mu}$ to get, on observing that $\mathbb{E}[n - X] = (1/R_0)\sum_j jp_j = \mu$ so that $\mathbb{E}[X/\mu] = n/\mu - 1$,

$$\sum_{j=1}^{n} p_j R_0^{(n-j)/\mu} = R_0 \sum_{j=1}^{n} q_j R_0^{(n-j)/\mu} = R_0 \mathbb{E}[a^X]$$

$$\geq R_0 a^{\mathbb{E}[X]} = R_0^{n/\mu}.$$

Hence, with $\theta = R_0^{1/\mu}$, we have

$$\theta^n - \sum_{j=1}^{n} \theta^{n-j} p_j \leq 0,$$

that is,

$$\sum_{j=1}^{n} \theta^{-j} p_j \geq 1,$$

from which we recall that it follows that $\lambda \geq R_0^{1/\mu}$. If $\lambda > 1$, this gives

$$T = \frac{\log R_0}{\log \lambda} \leq \frac{\log R_0}{\log R_0^{1/\mu}} = \mu.$$

For $\lambda < 1$, we have

$$T = \frac{\log(1/R_0)}{\log(1/\lambda)} \geq \frac{\log(1/R_0)}{\log(1/R_0^{1/\mu})} = \mu.$$

To compare T with A, observe that $1 = \sum_j \lambda^{-j} p_j = R_0 \sum_j \lambda^{n-j} q_j$, that is,

$$R_0 = \frac{1}{\sum_{j=1}^{n} \lambda^{-j} q_j} = \frac{1}{\mathbb{E}[e^{-\ell X}]},$$

where $\ell = \log \lambda$ and X is given by $\mathbb{P}(X = j) = q_j$. Hence,

$$T = \frac{-\log \mathbb{E}[e^{-\ell X}]}{\ell}.$$

With this notation we also have

$$A = \sum_{j=1}^{n} j\lambda^{-j} p_j = \frac{\sum_{j=1}^{n} j\lambda^{-j} p_j}{\sum_{j=1}^{n} \lambda^{-j} p_j} = \frac{\mathbb{E}[Xe^{-\ell X}]}{\mathbb{E}[e^{-\ell X}]}.$$

It follows that if $\lambda > 1$ (i.e., $\ell > 0$), then $T - A$ has the same sign as

$$-\mathbb{E}[e^{-\ell X}] \log \mathbb{E}[e^{-\ell X}] - l\mathbb{E}[Xe^{-\ell X}],$$

which, on using Jensen's inequality on the convex function $x \rightarrow x \log x$ and taking $x = e^{-\ell x}$, is seen to be at least

$$-\mathbb{E}[-\ell Xe^{-\ell X}] - \ell\mathbb{E}[Xe^{-\ell X}] = 0.$$

For $\ell < 0$, take $m = -\ell$ and observe that $T - A$ has the sign of

$$m\mathbb{E}[Xe^{mX}] - \mathbb{E}[e^{mX}] \log \mathbb{E}[e^{mX}],$$

which by an analogous argument is at most 0. This finishes the proof.

There are several remarks that are worthwhile to make, outlined below.

Remarks

1. If all mothers produce offspring at a given fixed age (i.e., $f_j > 0$ for only one j), then $p_j > 0$ for only that j; in that case, $\lambda = p_j^{1/j}$ and it is easy to see that $T = A = \mu = j$.

2. If p_j is of the form $p_j = \gamma q_j$ (e.g., if the fecundity is constantly equal to γ and $q_j = S_{j-1}$), then μ is trivially independent of γ, whereas clearly A is strictly decreasing as λ is strictly increasing in γ.

3. If $p_j = \gamma a^j$ (e.g., with constant fecundity and constant survival rate), then A is independent of a. To see this, note that the Euler-Lotka equation in this case reads

$$\sum_{j=1}^{n} \left(\frac{a}{\theta}\right)^j = \frac{1}{\gamma}.$$

Let c be the unique positive real solution to $\sum_j c^j = 1/\gamma$. Then $\lambda = a/c$ and hence

$$A = \gamma \sum_{j=1}^{n} j\lambda^{-j} a^j = \gamma \sum_{j=1}^{n} jc^j,$$

which is independent of a.

4. The difference between the three measures of generation time can sometimes be extreme. Take, for example, $p_1 = p_n = \gamma$ and $p_j = 0$ for all other j and let γ grow. Then μ is constantly equal to $(n + 1)/2$. However,

$\lambda/\gamma \to 1$ as $\gamma \to \infty$. This follows from plugging in γ and $(1 + \epsilon)\gamma$, respectively, in the characteristic equation and finding that the left-hand side is negative in the former case and positive in the latter for sufficiently large γ. From this we see that $T = \log(2\gamma)/\log(\gamma)$ plus a factor that converges to 0 as $\gamma \to \infty$. This in turn also converges to 1. Since $T \to 1$, theorem 1 implies that also $A \to 1$ as $\gamma \to \infty$.

5. If one regards T, μ, and A as functions of λ, then $T'(1) = (A'(1) + \mu'(1))/2$ regardless of the underlying change of the p_j's. To prove that, consider the three measures as functions of λ, which in turn converges to 1 as $p'_j \to p_j$, $j = 1, \ldots, n$, where $\sum p_j = 1$. Write $p'_j = p_j + \epsilon r_j$, where we without loss of generality assume that $\sum r_j = 1$ and consider $\epsilon \to 0$. Now λ changes as a function of ϵ, but it is more convenient to turn the tables and regard ϵ as a function of λ. The two quantities relate as

$$\sum \lambda^{-j}(p_j + \epsilon r_j) = 1,$$

which gives

$$\epsilon(\lambda) = \frac{1 - \sum \lambda^{-j} p_j}{\sum \lambda^{-j} r_j}.$$

Differentiating we find after some algebra (using that $\epsilon(1) = 0$ and $\sum p_j = \sum r_j = 1$) that

$$\epsilon'(1) = P_1$$

and

$$\epsilon''(1) = (2R_1 - 1)P_1 - P_2,$$

where $P_1 = \sum j p_j$, $R_1 = \sum j r_j$, and $P_2 = \sum j^2 p_j$. Now μ regarded as a function of λ reads

$$\mu(\lambda) = \frac{P_1 + R_1 \epsilon(\lambda)}{1 + \epsilon(\lambda)}.$$

The chain rule then gives

$$\mu'(\lambda) = \frac{R_1 \epsilon'(\lambda)}{1 + \epsilon(\lambda)} - \frac{(P_1 + R_1 \epsilon(\lambda))\epsilon'(\lambda)}{(1 + \epsilon(\lambda))^2},$$

which gives in turn

$$\mu'(1) = P_1 R_1 - P_1^2.$$

Using the chain rule on

$$A(\lambda) = \sum j \lambda^{-j}(p_j + \epsilon(\lambda)r_j)$$

leads to

$$A'(1) = P_1 R_1 - P_2.$$

Next, writing $\lambda = 1 + \rho$ and using Taylor's formula twice,

$$T(\lambda) = T(1 + \rho) = \frac{\log(1 + \epsilon(\rho))}{\log(1 + \rho)}$$

$$= \frac{\log(1 + P_1\rho + (1/2)((2R_1 - 1)P_1 - P_2))}{\log(1 + \rho)} + O(\rho^2)$$

$$= P_1 + \left(P_1 R_1 - \frac{1}{2}P_1^2 - \frac{1}{2}P_2\right)\rho + O(\rho^2).$$

Since $T(1) = P_1$, we can read off from this that

$$T'(1) = P_1 R_1 - \frac{1}{2}P_1^2 - \frac{1}{2}P_2 = \frac{\mu'(1) + A'(1)}{2}$$

as desired. (Many of the above computations have been completed with symbol-manipulating software, such as Maple.)

Literature Cited

Bakker, V. J., M. E. Finkelstein, J. D'Elia, D. F. Doak, and S. Kirkland. 2022. Genetically based demographic reconstructions require careful consideration of generation time. Current Biology 32:R356–R357. https://doi.org/10.1016/j.cub.2022.03.048.

Besenbacher, S., C. Hvilsom, T. Marques-Bonet, T. Mailund, and M. H. Schierup. 2019. Direct estimation of mutations in great apes reconciles phylogenetic dating. Nature Ecology and Evolution 3:286–292.

Bielby, J., G. M. Mace, O. R. Bininda-Emonds, M. Cardillo, J. L. Gittleman, K. E. Jones, C. D. Orme, and A. Purvis. 2007. The fast-slow continuum in mammalian life history: an empirical reevaluation. American Naturalist 169:748–757.

Bienvenu, F., and S. Legendre. 2015. A new approach to the generation time in matrix population model. American Naturalist 185:834–843.

Bird, J. P., R. Martin, H. R. Akçakaya, J. Gilroy, I. J. Burfield, S. T. Garnett, A. Symes, J. Taylor, Ç. H. Şekercioğlu, and S. H. M. Butchart. 2020. Generation lengths of the world's birds and their implications for extinction risk. Conservation Biology 34:1252–1261. https://doi.org/10.1111/cobi.13486.

Caswell, H. 2001. Matrix population models: construction, analysis, and interpretation. 2nd ed. Sinauer, Sunderland, MA.

Chao, L., and D. E. Carr. 1993. The molecular clock and the relationship between population size and generation time. Evolution 47:688–690.

Charlesworth, B. 1994. Evolution in age-structured populations. 2nd ed. Cambridge University Press, Cambridge.

Chittleborough, R. G. 1965. Dynamics of two populations of the humpback whale, *Megaptera novaeangliae* (Borowski). Australian Journal of Marine and Freshwater Research 16:33–128.

Coale, A. J. 1972. The growth and structure of human populations—a mathematical investigation. Princeton University Press, Princeton, NJ.

Cooke, R. S. C., T. C. Gilbert, P. Riordan, and D. Mallon. 2018. Improving generation length estimates for the IUCN Red List. PLoS ONE 13:e0191770. https://doi.org/10.1371/journal.pone.0191770.

Cousins, K., and J. Cooper. 2000. The population biology of the black-footed albatross in relation to mortality caused by long-line fishing. Western Pacific Regional Fishery Management Council, Honolulu, HI.

Dierickx, E. G., A. J. Shultz, F. Sato, T. Hiraoka, and S. V. Edwards. 2015. Morphological and genomic comparisons of Hawaiian and Japanese black-footed albatrosses (*Phoebastria nigripes*). Evolutionary Applications 8:662–678.

Dublin, L. I., and A. J. Lotka. 1925. On the true rate of natural increase. Journal of the American Statistical Association 20:305–339. https://doi.org/10.1080/01621459.1925.10503498.

Easteal, S. 1985. Generation time and the rate of molecular evolution. Molecular Biology and Evolution 2:450–453.

Fedoseev, G. A. 1975. Ecotypes of the ringed seal (*Pusa hispida* Schreber, 1777) and their reproductive capabilities. Rapports et procès-verbaux des réunions Conseil International pour l'Exploration de la Mer 169:156–160.

Fenner, J. 2005. Cross-cultural estimation of the human generation interval for use in genetics-based population divergence studies. American Journal of Physical Anthropology 128:415–423.

Figuet, E., B. Nabholz, M. Bonneau, E. M. Carrio, K. Nadachowska-Brzyska, H. Ellegren, and N. Galtier. 2016. Life history traits, protein evolution, and the nearly neutral theory in amniotes. Molecular Biology and Evolution 3:1517–1527.

Fujiwara, M., and J. B. Diaz-Lopez. 2017. Constructing stage-structured matrix population models from life tables: comparison of methods. PeerJ 5:e3971.

Gao, Z., M. J. Wyman, G. Sella, and M. Przeworski. 2016. Interpreting the dependence of mutation rates on age and time. PLoS Biology 14:e1002355. https://doi.org/10.1371/journal.pbio.1002355.

Haccou, P., P. Jagers, and V. A. Vatutin. 2005. Branching processes: variation, growth, and extinction of populations. Cambridge University Press, Cambridge.

Harding, K. C., T. Harkonen, and H. Caswell. 2002. The 2002 European seal plague: epidemiology and population consequences. Ecology Letters 5:727–732.

Harding, K. C., T. Harkonen, B. Helander, and O. Karlsson. 2007. Status of Baltic grey seals: population assessment and risk analysis. Nammco Scientific Publications 6:33–56.

Harkonen, T., K. C. Harding, S. Goodman, and K. Johannesson. 2005. Colonization history of the Baltic harbor seals: integrating archaeological, behavioural and genetic data. Marine Mammal Science 21:695–716.

Harkonen, T., K. C. Harding, and M. P. Heide-Jorgensen. 2002. Rates of increase in age-structured populations: a lesson from the European harbour seal. Canadian Journal of Zoology 80:1498–1510.

Holst, M., and I. Stirling. 2002. A comparison of ringed seal (*Phoca hispida*) biology on the east and west sides of the North Water Polynya, Baffin Bay. Aquatic Mammals 28:221–230.

IUCN (International Union for Conservation of Nature). 2006. Guidelines for using the IUCN Red List categories and criteria. Version 6.2. Prepared by the Standards and Petitions Working Group of the IUCN SSC Biodiversity Assessments Sub-Committee in December 2006.

———. 2012. Red List categories and criteria. 2nd ed., version 3.1. IUCN, Gland.

Jackson, J. A., C. E. Baker, M. Vant, D. J. Steel, L. Medrano-Gonzalez, and S. R. Palumbi. 2009. Big and slow: phylogenetic estimates of molecular evolution in baleen whales (suborder Mysticeti). Molecular Biology and Evolution 26:2427–2440.

Jagers, P. 1975. Branching processes with biological applications. Wiley, London.

Jensen, J. L. W. V. 1906. Sur les fonctions convexes et les inégalités entre les valeurs moyennes. Acta Mathematica 30:175–193. https://doi.org/10.1007/BF02418571.

Jonasson, J. 2022. Generation times. https://doi.org/10.5281/zenodo.6600015.

Kishino, H., H. Kato, F. Kasamatsu, and Y. Fujise. 1991. Detection of heterogeneity and estimation of population characteristics from the field survey data—1987/88 Japanese feasibility study of the Southern Hemisphere minke whales. Annals of the Institute of Statistical Mathematics 43:435–453.

Kjellqvist, S. A., T. Haug, and T. Oritsland. 1995. Trends in age-composition, growth and reproductive parameters of Barents Sea harp seals, *Phoca groenlandica*. ICES Journal of Marine Science 52:197–208.

Kong, A., M. L. Frigge, G. Masson, S. Besenbacher, P. Sulem, G. Magnusson, S. A. Gudjonsson, et al. 2012. Rate of de novo mutations and the importance of father's age to disease risk. Nature 488:471–475.

Kriebel, D., J. Tickner, P. Epstein, J. Lemons, R. Levins, E. L. Loechler, M. Quinn, R. Rudel, T. Schettler, and M. Stoto. 1981. The precautionary principle in environmental science. Canadian Journal of Zoology 59:966–981. https://doi.org/10.1289/ehp.01109871.

Lande, R. 1988. Demographic models of the northern spotted owl (*Strix occidentalis caurina*). Oecologica 75:601–607.

Laughlin, R. 1965. Capacity for increase: a useful population statistic. Journal of Animal Ecology 34:77–91.

Lebreton, J. D. 1996. Demographic models for subdivided populations: the renewal equation approach. Theoretical Population Biology 49:291–313.

Lehtonen, J., and R. Lanfear. 2014. Generation time, life history and the substitution rate of neutral mutations. Biology Letters 10:20140801. https://doi.org/10.1098/rsbl.2014.0801.

Leslie, P. H. 1966. The intrinsic rate of increase and the overlap of successive generations in a population of guillemots (*Uria aalge* pont.). Journal of Animal Ecology 35:291–231.

Li, H., and R. Durbin. 2011. Inference of human population history from individual whole-genome sequences. Nature 475:493–496.

Li, W. H., D. L. Ellsworth, J. Krushkal, B. H. J. Chang, and D. Hewett-Emmet. 1996. Rates of nucleotide substitution in primates and rodents and the generation-time effect hypothesis. Molecular Phylogenetics and Evolution 5:182–187.

Martin, A. P., and S. R. Palumbi. 1993. Body size, metabolic rate, generation time and the molecular clock. Proceedings of the National Academy of Sciences of the USA 90:4097–4091.

McLaren, I. A. 1958. The biology of the ringed seal (*Phoca hispida* Schreber) in the eastern Canadian arctic. Bulletin of the Fisheries Research Board of Canada no. 118.

Mooers, A. O., and P. H. Harvey. 1994. Metabolic rate, generation time and the rate of molecular evolution in birds. Molecular Phylogenetics and Evolution 3:344–350.

Nadachowska-Brzyska, K., C. Li, L. Smeds, G. J. Zhang, and H. Ellegren. 2015. Temporal dynamics of avian populations during Pleistocene revealed by whole-genome sequences. Current Biology 25:1375–1380.

Nei, M. 1987. Molecular evolutionary genetics. Columbia University Press, New York.

Nei, M., T. Maruyama, and R. Chakraborty. 1975. The bottleneck effect and genetic variability in populations. Evolution 29:1–10. https://doi.org/10.1111/j.1558-5646.1975.tb00807.x.

Nei, M., and N. Takahata. 1993. Effective population size, genetic diversity, and coalescence time in subdivided populations. Journal of Molecular Evolution 37:240–244.

Niel, C., and J. Lebreton. 2005. Using demographic invariants to detect overharvested bird populations from incomplete data. Conservation Biology 19:826–835.

Ohta, T., and M. Kimura. 1971. On the constancy of the evolutionary rate of cistrons. Journal of Molecular Evolution 1:18–25.

Palo, J. U., H. Hyvärinen, E. Helle, H. S. Mäkinen, and R. Väinölä. 2003. Postglacial loss of microsatellite variation in the landlocked Lake Saimaa ringed seal. Conservation Genetics 4:117–128.

Pastene, L. A., M. Goto, N. Kanda, A. N. Zerbini, D. Kerem, K. Watanabe, Y. Bessho, et al. 2007. Radiation and speciation of pelagic organisms during periods of global warming: the case of the common minke whale, *Balaenoptera acutorostrata*. Molecular Ecology 16:1481–1495.

Roman, J., and S. Palumbi. 2003. Whales before whaling in the North Atlantic. Science 301:508–510.

Romiguier, J., V. Ranwez, E. J. P. Douzery, and N. Galtier. 2010. Contrasting GC-content dynamics across 33 mammalian genomes: relationship with life-history traits and chromosome sizes. Genome Research 20:1001–1009.

Sæther, B. E., R. Lande, S. Engen, H. Weimerskirch, M. Lillegård, and R. Altwegg. 2005. Generation time and temporal scaling of bird population dynamics. Nature 436:99–102.

Sarich, V. M., and A. C. Wilson. 1973. Generation time and genomic evolution in primates. Science 79:1144–1177.

Scally, A., and R. Durbin. 2012. Revising the human mutation rate: implications for understanding human evolution. Nature Reviews Genetics 13:745–753.

Silva, W. T. A. F., E. Bottagisio, T. Härkönen, A. Galatius, M. T. Olsen, and K. C. Harding. 2021. Risk for overexploiting a seemingly stable seal population: influence of multiple stressors and hunting. Ecosphere 2:e03343. https://doi.org/10.1002/ecs2.3343.

Skaug, H. J. 2001. Allele-sharing methods for estimation of population size. Biometrics 57:750–756.

Smith, T. G. 1973. Population dynamics of the ringed seal in the Canadian eastern Arctic. Bulletin of the Fisheries Research Board of Canada no. 181.

Smith, T. G., and M. O. Hammill. 1981. Ecology of the ringed seal, *Phoca hispida*, in its fast ice breeding habitat. Canadian Journal of Zoology 59:966–981.

Staerk, J., D. A. Conde, V. Ronget, J. F. Lemaitre, J. M. Gaillard, and F. Colchero. 2019. Performance of generation time approximations for extinction risk assessments. Journal of Applied Ecology 56:1436–1446.

Stoffel, M. A., E. Humble, A. J. Paijmans, K. Acevedo-Whitehouse, B. L. Chilvers, B. Dickerson, F. Galimberti, et al. 2018. Demographic histories and genetic diversity across pinnipeds are shaped by human exploitation, ecology and life-history. Nature Communications 9:4836.

Taylor, J. L., J. P. G. Debost, and S. U. Morton. 2019. Paternal-age-related de novo mutations and risk for five disorders. Nature Communications 10:3043. https://doi.org/10.1038/s41467-019-11039-6.

Weir, J. T., and D. Schluter. 2008. Calibrating the avian molecular clock. Molecular Ecology 17:2321–2318. https://doi.org/10.1111/j.1365-294X.2008.03742.x.

Wu, C. I., and W. H. Li. 1985. Evidence for higher rates of nucleotide substitution in rodents than in man. Proceedings of the National Academy of Sciences of the USA 82:1741–1745.

Wu, J., T. Yonezawa, and H. Kishino. 2021. Evolution of reproductive life history in mammals and the associated change of functional constraints. Genes 12:740.

Associate Editor: Robin E. Snyder
Editor: Jennifer A. Lau

KJOEKKENMOEDDING

"Each heap, too, is covered with a deposit of earth and vegetable mould, of variable thickness, and in some cases, as at Frenchman's Bay, supporting a growth of forest trees, though these were nowhere of such size as to indicate that they had lived a century." From "An Account of Some Kjœkkenmœddings, or Shell-Heaps, in Maine and Massachusetts" by Jeffries Wyman (*The American Naturalist*, 1868, 1:561–584).